ELSEVIER

Biochimica et Biophysica Acta 1467 (2000) 219–226

BIOCHIMICA ET BIOPHYSICA ACTA

BBA

www.elsevier.com/locate/bba

Optical characterization of liposomes by right angle light scattering and turbidity measurement

Katsumi Matsuzaki *, Osamu Murase, Ken'ichi Sugishita, Shuji Yoneyama, Ken'ya Akada, Mayu Ueha, Akemi Nakamura, Satoe Kobayashi

Graduate School of Biostudies and Graduate School of Pharmaceutical Sciences, Yoshida-Shimoadachi-cho 46-29, Sakyo-ku, Kyoto 606-8501, Japan

Received 16 November 1999; received in revised form 16 March 2000; accepted 13 April 2000

Abstract

Liposomes have frequently been used as models of biomembranes or vehicles for drug delivery. However, the systematic characterization of lipid vesicles by right angle light scattering and turbidity has not been carried out despite the usefulness of such studies for size estimation. In this study, liposomes of various sizes were prepared by sonication and extrusion. The mean cumulant radii of the vesicles were determined by dynamic light scattering. The lamellarities were estimated based on fluorescence quenching of *N*-(7-nitrobenz-2-oxa-1,3-diazol-4-yl)dipalmitoyl-L-α-phosphatidylethanolamine by sodium dithionite. Right angle light scattering intensity and optical density at 436 nm per unit lipid concentration were measured as a function of vesicle radius. With a vesicle radius ≤100 nm, the optical parameters could be well explained by the Rayleigh–Gans–Debye theory in which the liposomes were modeled as homogenous spheres with mean refractive indices determined by the volume fractions of lipids in vesicles.

Keywords: Rayleigh–Gans–Debye equation; Lamellarity; Refractive index

1. Introduction

Liposomes have widely been used as models of biomembranes or vehicles for drug delivery [1,2]. The determination and control of vesicle size are critically important for several reasons. The liposome radius or curvature is known to significantly affect the physicochemical properties of lipid bilayers. For example, small unilamellar vesicles (SUV) suffering from large curvature strains show a broader gel to liquid crystalline phase transition [3] and stronger interactions with peptides compared with liposomes of larger radii [4,5]. In pharmaceutical applications, drug encapsulation efficiency and in vivo behavior are highly dependent on vesicle size [6,7].

The size distribution of liposomes is commonly determined by dynamic light scattering (DLS) and electron microscopy. These techniques are, however,

Abbreviations: DLS, dynamic light scattering; egg PC, egg yolk L-α-phosphatidylcholine; LEV, large extruded vesicles; LUV, large unilamellar vesicles; MLV, multilamellar vesicles; NBD, *N*-7-nitrobenz-2-oxa-1,3-diazol-4-yl; NBD-PE, *N*-(7-nitrobenz-2-oxa-1,3-diazol-4-yl)dipalmitoyl-L-α-phosphatidylethanolamine; NBD-PC, 1-palmitoyl-2-[6-((7-nitrobenz-2-oxa-1,3-diazol-4-yl)amino)caproyl]-L-α-phosphatidylcholine; RGD, Rayleigh–Gans–Debye; SUV, small unilamellar vesicles

* Corresponding author. Fax: +81-75-761-2698;
E-mail: katsumim@pharm.kyoto-u.ac.jp

0005-2736/00/$ – see front matter
PII: S0005-2736(00)00223-6

time-consuming and therefore not appropriate for systems in which the particle size changes rapidly. Good examples are the aggregation, fusion and micellization of liposomes induced by peptides and other agents, e.g. polyethyleneglycol. In these cases, right angle light scattering [8–11] or turbidity [11–13] have often been continuously monitored using conventional spectrofluorimetry or spectrophotometry, respectively, as a measure of vesicle size. However, the interpretation of the results is not straightforward [8,11], even if liposomes are assumed to be ideal monodispersed spheres. First, light scattering and turbidity per se are known to be complicated oscillating functions dependent on both the particle size and wavelength of incident light. Second, liposomes are not optically homogenous particles.

As summarized by Kerker [14], Rayleigh scattering is a theory to explain light scattering by particles much smaller than the wavelength of incident light. The rigorous light scattering theory for spheres of arbitrary size was later developed by Mie. The simpler Rayleigh–Gans–Debye (RGD) approximation can be used under certain conditions (see Section 2).

Many studies, both theoretical and experimental, have been performed to clarify the relationships among vesicle size, light wavelength and optical properties. The total volume of liposomes was found to be reciprocally proportional to turbidity at 450 nm [15]. Based on the Mie theory, Yoshikawa et al. showed that turbidity is reciprocally proportional to the two-thirds power of the volume by treating multilamellar vesicles (MLV) as optically homogenous spheres with an average refractive index estimated by the volume fraction of lipid in the vesicle [16]. In an earlier study, Chong and Colbow calculated the specific 90° light scattering intensity and turbidity as a function of vesicle size and aqueous radius in the framework of the RGD theory [17]. They not only explicitly took the multilamellar structure into account in the calculation, but also treated it as a thick single lipid shell with an averaged refractive index. They concluded that the latter approach could better explain experimental observations. Nir et al. reported theoretical considerations on light scattering by unilamellar vesicles based on the RGD theory [18].

For comparison between theories and experimental results, the characterization of lipid vesicles in terms of size and lamellarity is essential. Over the last several years, methods for these purposes have been developed. In this study, liposomes of controlled size distributions were prepared by the extrusion method [19]. The lamellarities of the vesicles were estimated using the chemical quenching of *N*-(7-nitrobenz-2-oxa-1,3-diazol-4-yl)dipalmitoyl-L-α-phosphatidylethanolamine (NBD-PE) by membrane-impermeable sodium dithionite [20]. The specific right angle light scattering and turbidity could be well explained by the RGD theory for vesicles smaller than 100 nm in radius if the vesicles were treated as optically homogenous spheres with average refractive indices.

2. Theory

The intensity of light scattered by a sphere is dependent on the ratio of the particle radius, R, to the wavelength of incident beam in the medium, λ. The size parameter, α, is defined by

$$\alpha = 2\pi R/\lambda \tag{1}$$

$$\lambda = \lambda_0/n_W \tag{2}$$

The wavelength of the incident beam in vacuum and the refractive index of the medium (water) are denoted by λ_0 and n_W, respectively. Rayleigh scattering occurs when $\alpha \ll 1$ [14]. In this study, we investigated light scattering by liposomes with radii of 15–150 nm at 436 nm where the refractive indices of both water (1.340) and lipid ($n_L = 1.497$) are known [17]. Therefore, the α values ranged from 0.3 to 3, which is out of the Rayleigh scattering regime. If the relative refractive index, $m = n_{particle}/n_W$, is close to unity and $\alpha^4 \leq 10$, light scattering by particles of any size and shape can be described by the RGD equation [14,21].

$$I(\theta) \propto N_P J(\theta) \tag{3}$$

$$J(\theta) = \left(\frac{\lambda^2}{4\pi^2}\right)\left(\frac{m^2-1}{m^2+2}\right)^2 \alpha^6 \left(\frac{1+\cos^2\theta}{2}\right) P(\theta) \tag{4}$$

$I(\theta)$ and $J(\theta)$ as functions of scattering angle, θ, represent scattering intensity and the Rayleigh ratio for unpolarized incident light of unit intensity, respec-

tively. The number of particles per cm^3 is denoted by N_P. $P(\theta)$ is called the form factor.

The turbidity or the optical density (OD)$\times$2.303 is expressed by

$$2.303\ \mathrm{OD} = 2\pi N_P \int_0^{\pi} J(\theta)\sin\theta\ \mathrm{d}\theta \quad (5)$$

2.1. Homogenous sphere model

Liposomes are treated as optically homogenous spheres with the average refractive index, n_{av}, calculated according to [16]

$$\frac{n_{av}^2-1}{n_{av}^2+2} = f\frac{n_L^2-1}{n_L^2+2} + (1-f)\frac{n_W^2-1}{n_W^2+2} \quad (6)$$

The volume fraction of lipid in the vesicle, f, can be estimated as follows.

$$f = \frac{N_T v_L}{\frac{4}{3}\pi R^3} \quad (7)$$

v_L (= 1.3 nm^3) is the volume occupied by a lipid molecule [22]. N_T is the total number of lipid molecules per vesicle, and can be determined by NBD-PE experiments, which give the fraction of lipid molecules exposed to the external aqueous phase, x.

$$x = 4\pi R^2/N_T A_L \quad (8)$$

A_L (= 0.68 nm^2) denotes the area per lipid [23]. Combining Eqs. 7 and 8, we obtain

$$f = 3v_L/RxA_L \quad (9)$$

The form factor for optically homogenous spheres is [14]

$$P(\theta) = \left[\frac{3(\sin u - u\cos u)}{u^3}\right]^2 \quad (10)$$

$$u = 2\alpha\sin(\theta/2) \quad (11)$$

N_P is calculated by

$$N_P = 10^{-3}N_A[L]/N_T = xA_L 10^{-3}N_A[L]/4\pi R^2 \quad (12)$$

The lipid concentration is denoted by [L] (M^{-1}). N_A is the Avogadro number.

2.2. Hollow sphere model

Lipid vesicles can also be viewed as hollow spheres with shells of refractive index n_L. The form factor was described by [24]

$$P(\theta = \left[\frac{3(\sin u - \sin ul - u\cos u + ul\cos ul)}{u^3(1-l^3)}\right]^2 \quad (13)$$

$$l = (R-l_B)/R \quad (14)$$

The bilayer thickness is expressed as l_B (= 4 nm). The samples could be considered as mixtures of unilamellar and bilamellar vesicles (see Section 4). A bilamellar vesicle is considered to be composed of two vesicles with larger radius, R, and smaller radius, $R-l_B-l_W$. l_W (= 3 nm) is the thickness of the interlamellar aqueous phase. The numbers of the larger vesicles including the unilamellar vesicles, N_L, and the smaller vesicles, N_S, per cm^3 are related to x by

$$x = \frac{N_L R^2}{N_L\{R^2 + (R-l_B)^2\} + N_S\{R-l_B-l_W)^2 + (R-2l_B-l_W)^2\}} \quad (15)$$

The lipid concentration, [L] (M^{-1}), is also connected to N_L and N_S.

$$[L]10^{-3}N_A = N_L\frac{4\pi[R^2 + (R-l_B)^2]}{A_L} + N_S\frac{4\pi[(R-l_B-l_W)^2 + (R-2l_B-l_W)^2]}{A_L} \quad (16)$$

Eqs. 15 and 16 yield the values of N_L and N_S for known x, [L] and R values. The light scattering intensity and the turbidity are calculated by

$$I(\theta) \propto N_L J_L(\theta) + N_L J_L(\theta) \quad (17)$$

$$2.303\ \mathrm{OD} = 2\pi[N_L\int_0^{\pi} J_L(\theta)\sin\theta\,\mathrm{d}\theta + N_S\int_0^{\pi} J_S(\theta)\sin\theta\,\mathrm{d}\theta] \quad (18)$$

$J_L(\theta)$ and $J_S(\theta)$ are $J(\theta)$ for the larger and the smaller vesicles, respectively. The above treatment is essentially the same as that described by Chong and Col-

bow [17], who explicitly calculated the form factor of the multishell structure.

3. Materials and methods

3.1. Materials

Egg yolk L-α-phosphatidylcholine (egg PC) was purchased from Sigma (St. Louis, MO, USA). NBD-PE and 1-palmitoyl-2-[6-((7-nitrobenz-2-oxa-1,3-diazol-4-yl)amino)caproyl]-L-α-phosphatidylcholine (NBD-PC) were obtained from Molecular Probes (Eugene, OR, USA) and Avanti Polar Lipids (Alabaster, AL, USA). Tris–HCl buffer (10 mM Tris/150 mM NaCl/1 mM EDTA, pH 7.0) was prepared from water distilled twice in a glass still.

3.2. Vesicle preparation

Egg PC containing 0.5 mol% NBD-PE was dissolved in chloroform and placed in a round-bottomed flask. The solvent was removed in a rotary evaporator. After drying under vacuum overnight, the residual lipid film was hydrated with Tris buffer and vortex-mixed. The suspension was subjected to five freeze-thaw cycles to produce MLV. The freeze-thaw procedure reduces the lamellarity of the vesicles [19]. SUV were obtained by sonicating the MLV for 20 min to clarity on ice under an atmosphere of N_2. Metal debris was removed by centrifugation. Large extruded vesicles (LEV) were prepared by extruding the MLVs five times through polycarbonate filters (0.6 μm pore size, LEV600). The vesicles were further extruded 10 times through two stacked filters with pore sizes of 0.05, 0.1, 0.2 or 0.4 μm (LEV50, LEV100, LEV200 and LEV400, respectively). The particle size was determined with a Photal laser particle analyzer LPA-3100 connected to a photon correlator LPA-3000. The vesicle radii were calculated by the cumulant method program provided by the manufacturer. The averages of at least three measurements are listed. The lipid concentration was determined in triplicate by phosphorus analysis.

3.3. Lamellarity

The fraction of the NBD–lipid exposed to the external aqueous phase was measured on the basis of fluorescence quenching by sodium dithionite [20]. The NBD-labeled vesicles (2.0 ml) were incubated for 10 min at 25°C. After 20 μl of 1 M sodium dithionite/1 M Tris had been added to the sample, NBD fluorescence was monitored on a Shimadzu RF-5000 spectrofluorometer with excitation and emission wavelengths of 450 nm and 530 nm, respectively. Fluorescence intensity, F, was normalized to the intensity prior to dithionite addition, F_0. The experiments were performed at least in duplicate.

3.4. Right angle light scattering and turbidity

The right angle light scattering intensities at various wavelengths were determined on the spectrofluorometer by simultaneously scanning the excitation and emission wavelengths (synchronous spectra). The turbidity at 436 nm was measured on a Shimadzu UV-265FW spectrophotometer using a 1 cm path length cuvette. During these optical experiments, the temperature was maintained at 25°C.

Table 1
Characterization of liposomes

Liposome	R (nm)	x_1	x_2	x	f	n_{av}	m
SUV	14.9	0.651	–	–	0.591	1.431	1.068
LEV50	35.9	0.559	0.343	0.470	0.340	1.392	1.038
LEV100	49.6	0.542	0.314	0.426	0.271	1.381	1.031
LEV200	76.5	0.527	0.289	0.354	0.212	1.372	1.024
LEV400	103.5	0.520	0.278	0.306	0.181	1.367	1.020
LEV600	142.4	0.514	0.270	0.260	0.155	1.363	1.017
LUV100	59.3	0.535	0.302	0.580	0.167	1.365	1.019

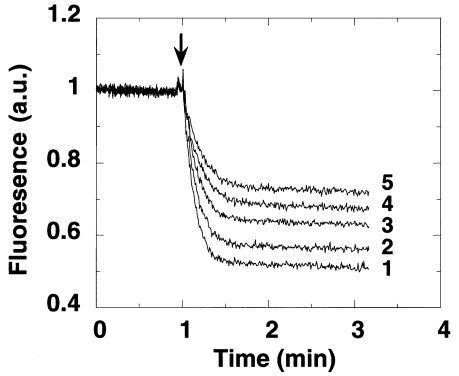

Fig. 1. Lamellarities of liposomes. Twenty μl of 1 M sodium dithionite/1 M Tris solution was injected into 2 ml of a suspension of egg PC vesicles doped with 0.5 mol% NBD-PE at 25°C (indicated by the arrow). Fluorescence intensity at 530 nm (excitation at 450 nm) was monitored. Traces: 1, LEV50; 2, LEV100; 3, LEV200; 4, LEV400; 5, LEV600.

4. Results and discussion

4.1. Characterization of vesicles

Lipid vesicles were characterized in terms of size and lamellarity. The cumulant radii, R, determined by DLS are summarized in Table 1. As reported [19], the average size of LEV100 was the same as that of the filter pores. LEV50 showed a larger radius than expected, whereas LEV200, LEV400 and LEV600 exhibited smaller sizes. The theoretical x values of unilamellar (x_1) and bilamellar (x_2) vesicles are also listed in Table 1.

$$x_1 = \frac{R^2}{R^2 + (R - l_B)^2} \tag{19}$$

$$x_2 = \frac{R^2}{R^2 + (R - l_B)^2 + (R - l_B - l_W)^2 + (R - 2l_B - l_W)^2} \tag{20}$$

To estimate the x values, we carried out the NBD–dithionite assay [20]. This method is based on the chemical quenching (reduction) of the fluorophore by the membrane-impermeable $S_2O_4^{2-}$ ion. Fig. 1 shows the time course of quenching, which was biphasic. The fast reduction in fluorescence intensity represents the reaction of the NBD groups in the outermost leaflets with the reducing ions in the external aqueous phase. The slow phase reflects the quenching of the fluorophores in the inner leaflets by slowly permeating ions [20]. In the slower step, fluorescence intensity decreased almost linearly with time (Fig. 1). The x values were estimated by $F(t \rightarrow 0)/F_0$, where $F(t \rightarrow 0)$ represents the F value linearly extrapolated to $t \rightarrow 0$, and summarized in Table 1. The x values of smaller vesicles were closer to the corresponding x_1 values, whereas that of the largest LEV600 was almost identical to x_2. Accordingly, we assumed that these were mixtures of unilamellar and bilamellar vesicles. These results were comparable to those in the original paper [19], although the x values of LEV50 and LEV100 in the present study were somewhat smaller. More extensive extrusion (31 times) through a 0.1 μm pore filter yielded large unilamellar vesicles (LUV) 100 (Table 1). The observed x value of SUV (0.31) was reproducibly much smaller than the expected value ($x_1 = 0.65$). The lamellarity of SUV was also determined using another probe NBD-PC, which gave an extremely large x value of

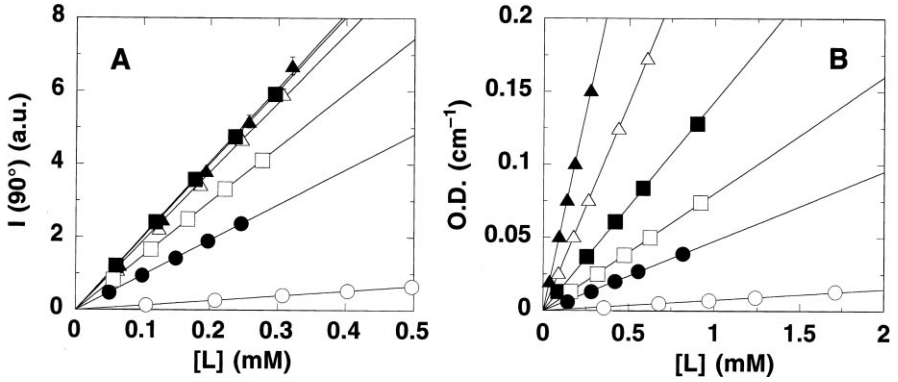

Fig. 2. Dependence of optical parameters on lipid concentration. (A) Right angle light scattering intensity (arbitrary unit) and (B) OD at 436 nm are plotted as a function of lipid concentration. Symbols: ○, SUV; ●, LEV50; □, LEV100; ■, LEV200; △, LEV400; ▲, LEV600. Linear regression lines are shown ($r^2 > 0.998$).

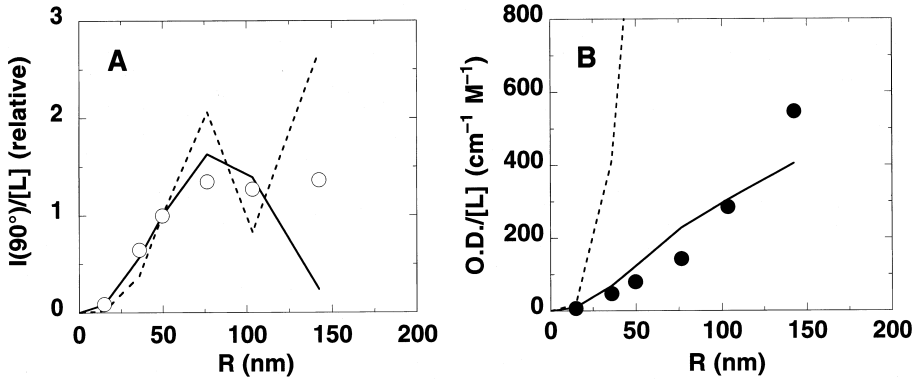

Fig. 3. Dependence of optical parameters on vesicle size. The slopes of the lines in Fig. 2A,B are shown by open and closed circles, respectively, against the cumulant radii, R, of the vesicles determined by DLS. The solid and dotted lines are theoretical values calculated by the homogenous sphere model and the hollow sphere model, respectively. In (A), the values are normalized relative to those for LEV100.

ca. 0.8. These strange results were probably due to asymmetric transbilayer distribution of lipids in sonicated vesicles [25]. It is well known that packing constraints do not allow SUV to have oligolamellar structures. Therefore, we reasonably assumed $x = x_1$.

4.2. Right angle light scattering

The right angle light scattering intensity, $I(90°)$, at 436 nm is plotted as a function of lipid concentration in Fig. 2A. Signals could be obtained at lipid concentrations ($\sim$0.2 mM) lower than in the turbidity measurement (Fig. 2B, $\sim$1 mM). The intensity was proportional to lipid concentration ($r^2 \geq 0.998$), indicating the absence of any effects due to multiple scattering. The slope, which was normalized to the value for LEV100, is plotted against R (Fig. 3A, open circles). $I(90°)$/[L] increased with R until $R = 75$ nm. At larger R values, this parameter was slightly but significantly decreased and then increased again (see also Fig. 5).

The position of the maximum was dependent on the wavelength of the incident light. The maxima appeared around 50 nm (open circles) and 120 nm (closed circles) at light wavelengths of 250 and 600 nm, respectively (Fig. 5). That is, the maximum was observed when $R \sim 0.2\lambda_0$.

The theoretical relative $I(90°)$/[L] values were calculated based on the two models described in the Section 2, and shown in solid and dotted lines in Fig. 3A. Table 1 includes the n_{av} values used in the homogenous sphere model (solid line). This model

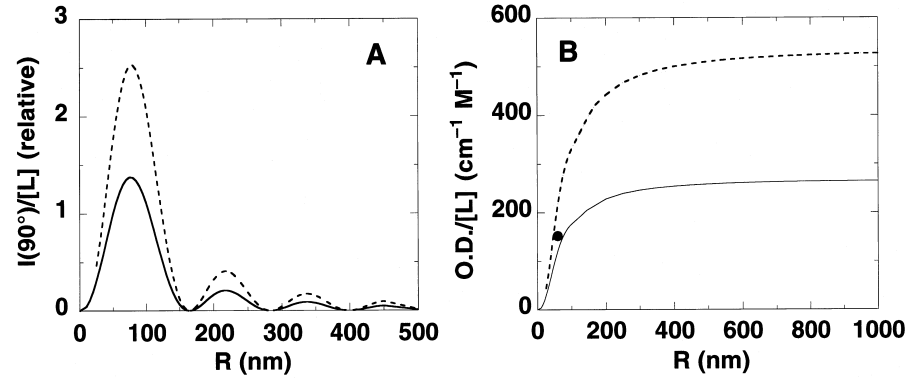

Fig. 4. Simulation of optical properties. Specific light scattering (A) and specific OD (B) at 436 nm are simulated by the homogenous sphere model. The solid and dotted curves are for unilamellar and bilamellar vesicles, respectively. In (A), the values are normalized against that for unilamellar vesicles with $R = 50$ nm. The observed OD/[L] value of LUV100 is shown in (B) (●).

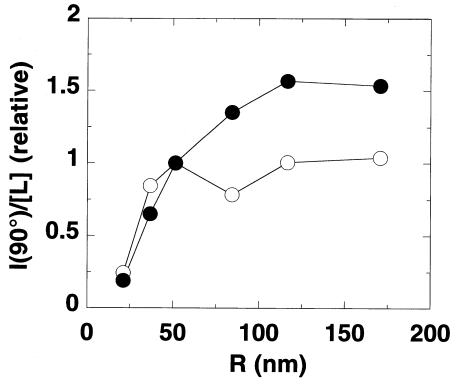

Fig. 5. Dependence of light scattering on the wavelength of incident light. Specific 90° light scattering intensities at 250 nm (open circles) and 600 nm (closed circles) are plotted as a function of R. The values are normalized relative to those for LEV100.

described the $I(90°)/[L]$ vs. R relationship in the range $R \leq 100$ nm. The fit by the hollow sphere model (dotted line) was poorer.

4.3. Turbidity

The OD value at 436 nm was also proportional to [L] in the concentration range investigated (Fig. 2B). The slope was plotted as a function of R in Fig. 3B (closed circles). In contrast to 90° light scattering, the slope increased monotonously with vesicle radius. The theoretical values were also indicated by solid and dotted lines in the figure. The integration in Eq. 5 was performed numerically using Mathematica software (Wolfram Research). The observed OD/[L] values were again much better reproduced by the homogenous sphere model (solid line).

4.4. Simulation

These results indicated that the homogenous sphere model suitably describes both right angle light scattering and turbidity of oligolamellar vesicles with $R \leq 100$ nm. Therefore, simulations were carried out for homogenous spherical unilamellar vesicles (solid lines) and bilamellar vesicles (dotted lines) using this model in Fig. 4. Right angle light scattering (Fig. 4A) is an oscillating function of R with progressively attenuated amplitude. The first largest maximum around 75 nm corresponded to the maximum shown in Fig. 3A. Note that the maximal R value for the bilamellar vesicles was slightly shifted to a larger value than that for the unilamellar vesicles. The intensity of the bilamellar vesicles was less than, but at larger R close to, twice that of the unilamellar vesicles. According to the simulation shown in Fig. 4A, light scattering should significantly decrease at R values larger than 75 nm, even if size distribution is taken into account. The observed intensity was, however, only slightly decreased, and then increased again (Fig. 3A and Fig. 5). There seemed to be several reasons for this. First, the RGD approximation holds only when $\alpha^4 \leq 10$, which was fulfilled for vesicles smaller than LEV200. Second, the coexistence of MLV may also contribute to the large light scattering. Indeed, the x value for LEV600 was somewhat larger than x_2 (Table 1), indicating the significant presence of vesicles with lamellarity larger than two. Furthermore, larger flexible vesicles may not be considered as spheres.

The OD/[L] ratio at 436 nm for unilamellar vesicles is a saturating function of R, and sensitive to R only below 200 nm. The value of the bilamellar vesicles was again less than twice that of the unilamellar vesicles. The observed value of LUV100 approximately fell on the theoretical curve for unilamellar vesicles. The predicted OD/[L] value for LUV100 using the hollow sphere model was much larger (>2000).

5. Conclusion

We demonstrated that right angle light scattering and turbidity of uni- and oligolamellar liposomes with radii smaller than 100 nm can be reasonably explained by the RGD theory assuming that the vesicles are optically homogenous spheres with average refractive indices determined by the volume fraction of lipid in the vesicle. It should be noted that the hollow sphere model, which was not applicable, also took oligolamellar structures into account explicitly. These results suggest that the vesicles do not optically behave like solid particles because of thermal fluctuations. The RGD theory is valid only when $m \approx 1$, which was fulfilled (Table 1). The fitting quality might be improved if the size distribution of liposomes was taken into consideration. However, its precise determination is difficult. For example, the

size distribution of a given sample by the DLS histogram method differs between measurements. Size measurement by electron microscopy is time-consuming and requires collection of huge numbers of vesicles. In contrast, the cumulant radii used here were reproducibly measurable and gave rough estimates of optical parameters.

Turbidity, although less sensitive (Fig. 1), is superior to light scattering for several reasons. Right angle light scattering presents more complication than turbidity measurements, and all other things being equal, may be less reliable (Fig. 3). This also limits the usable R range. Light scattering intensity is a monotonous function of R until $R=100$ even if a wavelength of 600 nm is used (Fig. 5). That is, fusion of only four LEV100 can be monitored as an increase in light scattering. In contrast, turbidity can follow fusion of up to 20 vesicles ($R\approx 200$ nm). Furthermore, light scattering could have artifacts not only from multiple scattering but also from inner-filter type effects. Finally, it should be stressed that optical measurements provide a good estimate of vesicle size only if the lamellarity is simultaneously determined.

References

[1] D.D. Lasic, in: Liposomes: from Physics to Applications, Elsevier, Amsterdam, 1993.
[2] D.D. Lasic and D. Papahadjopoulos, in: Medical Applications of Liposomes, Elsevier, Amsterdam, 1998.
[3] M.P. Sheetz, S.I. Chan, Biochemistry 11 (1972) 4573–4581.
[4] K. Matsuzaki, Y. Takaishi, T. Fujita, K. Miyajima, Colloid Polym. Sci. 269 (1991) 604–611.
[5] G. Beschiaschvili, J. Seelig, Biochemistry 31 (1992) 10044–10053.
[6] A. Nagayasu, K. Uchiyama, T. Nishida, Y. Yamagiwa, Y. Kawai, H. Kiwada, Biochim. Biophys. Acta 1278 (1996) 29–34.
[7] K. Uchiyama, A. Nagayasu, Y. Yamagiwa, T. Nishida, H. Harashima, H. Kiwada, Int. J. Pharm. 121 (1995) 196–203.
[8] K. Matsuzaki, M. Nakayama, M. Fukui, A. Otaka, S. Funakoshi, N. Fujii, K. Bessho, K. Miyajima, Biochemistry 32 (1993) 11704–11710.
[9] K. Matsuzaki, S. Yoneyama, N. Fujii, K. Miyajima, K. Yamada, Y. Kirino, K. Anzai, Biochemistry 36 (1997) 9799–9806.
[10] K. Matsuzaki, K. Sugishita, N. Ishibe, M. Ueha, S. Nakata, K. Miyajima, R.M. Epand, Biochemistry 37 (1998) 11856–11863.
[11] A.-R. Viguera, A. Alonso, F.M. Goñi, Colloids Surf. B 3 (1995) 263–270.
[12] K. Hong, V.D. Vacquir, Biochemistry 25 (1986) 543–549.
[13] A. Kitamura, T. Kiyota, M. Tomohiro, A. Umeda, S. Lee, T. Inoue, G. Sugihara, Biophys. J. 76 (1999) 1457–1468.
[14] M. Kerker, in: S. Ross (Ed.), Chemistry and Physics of Interfaces-II, American Chemical Society, Washington, DC, 1971, pp. 171–186.
[15] A.D. Bangham, J. de Gier, G.D. Greville, Chem. Phys. Lipids 1 (1967) 225–246.
[16] W. Yoshikawa, H. Akutsu, Y. Kyogoku, Biochim. Biophys. Acta 735 (1983) 397–406.
[17] C.S. Chong, K. Colbow, Biochim. Biophys. Acta 436 (1976) 260–282.
[18] S. Nir, J. Bentz, J. Wilschut, N. Duzgunes, Prog. Surf. Sci. 13 (1983) 1–124.
[19] L.D. Mayer, M.J. Hope, P.R. Cullis, Biochim. Biophys. Acta 858 (1986) 161–168.
[20] J.C. McIntyre, R.G. Sleight, Biochemistry 30 (1991) 11819–11827.
[21] W.J. Pangonis, W. Heller, N.A. Economou, J. Chem. Phys. 34 (1961) 960–970.
[22] H.I. Petrache, S. Tristram-Nagle, J.F. Nagle, Chem. Phys. Lipids 95 (1998) 83–94.
[23] G. Beschiaschvili, J. Seelig, Biochemistry 29 (1990) 10995–11000.
[24] R. Pecora, S.R. Aragón, Chem. Phys. Lipids 13 (1974) 1–10.
[25] D.M. Michaelson, A.F. Horwitz, M.P. Klein, Biochemistry 12 (1973) 2637–2645.